



Title	Construction of storage, remote afterloader, and treatment facility for californium-252 medical sources, and radiation protection survey
Author(s)	尾内, 能夫; 入船, 寅二; 都丸, 穎三 他
Citation	日本医学放射線学会雑誌. 1978, 38(7), p. 643-653
Version Type	VoR
URL	<a href="https://hdl.handle.net/11094/15155">https://hdl.handle.net/11094/15155</a>
rights	
Note	

*The University of Osaka Institutional Knowledge Archive : OUKA*

<https://ir.library.osaka-u.ac.jp/>

The University of Osaka

Construction of storage, remote afterloader, and treatment facility for  
californium-252 medical sources, and radiation protection survey

Yoshio Onai, Toraji Irfune, Teizo Tomaru and Isao Uchida

Department of Physics, Cancer Institute, Tokyo

Akira Tsuya and Koichi Kaneta

Department of Radiology, Cancer Institute Hospital, Tokyo

*Research Code No.:* 601

*Key Words:* *Californium-252, Remote afterloader, Radiation protection,  
Storage container, Shielded facility*

医療用  $^{252}\text{Cf}$  線源の貯蔵容器, 遠隔操作式アフターローダ  
および照射施設の製作と放射線防護のための測定

癌研究会癌研究所物理部

尾内 能夫 入船 寅二 都丸 穎三 内田 獻

癌研究会附属病院放射線科

津屋 旭 金田 浩一

(昭和53年2月20日受付)

(昭和53年3月17日最終原稿受付)

米国エネルギー局から貸与される管3本, セル10本, シードアセンブリ16本, 計約100 $\mu\text{g}$  の $^{252}\text{Cf}$ の貯蔵容器兼アフターローディング装置および照射治療施設を設計製作した。アフターローディング装置は20 $\mu\text{g}$  管3本と他の任意の線源一つを使用できる4チャンネルとし, 手動遠隔操作式である。照射施設は, 貯蔵室および水槽衝立て区画された二つの照射ベッドルームと操作兼準備室で構成されている。一つのベッドは遠隔操作式腔内照射用, 他のベッドは組織内照射用で, いずれも移動可能な水槽で遮蔽されている。貯蔵容器は円筒型で, 中央部に線源格納部がある。その周りを2cmの鉛で, その外側を45cmのパラフィンで,

更に最外側を2cmの鉛で遮蔽してある。線源格納部には線源を個別に収納できる各種のホルダーが用意されている。遠隔操作式アフターローダーとして使用するときには, それ用の線源格納部が設けられている。貯蔵時の貯蔵容器周辺および照射時の照射室内外における中性子線とガソマ線の漏洩線量の計算値と実測値を比較した。貯蔵容器では Stoddard らの球状遮蔽の計算法が適用できるが, 衝立式の板状遮蔽では, 床, 天井, 壁等からの散乱中性子線が混入するので, 特に低線量域で, 球状遮蔽の計算値より著しく大きな漏洩線量がみられる場合があるから注意を要する。

### Introduction

From the point of view of dose distribution, interstitial and intracavitary therapy using  $^{252}\text{Cf}$  sources

or  $\gamma$ -emitting sources offers considerable advantages over external neutron or  $\gamma$ -ray therapy. This method of irradiation, however, is associated with difficult radiation protection problems, not only during the application and removal of the radiation sources, but also in the nursing care of the patient during the course of treatment. To reduce these disadvantages, the so-called afterloading procedures have been developed.<sup>1-9)</sup> By using this procedure a considerable reduction of the radiation exposure can be achieved during the application and removal of the sources. However, afterloading does not help in reducing the exposure of the nursing staff at all. To reduce their exposure, bedside shielding and appropriate nursing procedures may be required.

This paper describes the design and construction of a shielded facility for storage and treatment of up to about 100  $\mu\text{g}$  of  $^{252}\text{Cf}$  seed assemblies, afterloading cells and tubes, and a remote afterloader for  $^{252}\text{Cf}$  tubes, and radiation protection survey of the completed facility.

### Design and Construction of Facility

#### 1. Location and arrangement of facilities

The facility in the Cancer Institute Hospital, Tokyo, is located in a first floor room at one end of a ward reserved for brachytherapy patients. The facility includes a storage room for  $^{252}\text{Cf}$  sources, two ward rooms for treatment with a remote afterloader and seed assemblies, and a handling and control room for the preparation of the seed assemblies and operation of the remote afterloader. The two ward rooms for patients and the handling room are separated by three 20-cm thick water-filled shields which are constructed of iron tanks, as shown in Figs. 1, 2, and 3.

#### 2. Patient bed

The patient bed is shielded by a movable water-filled iron tank which is mounted on rollers and

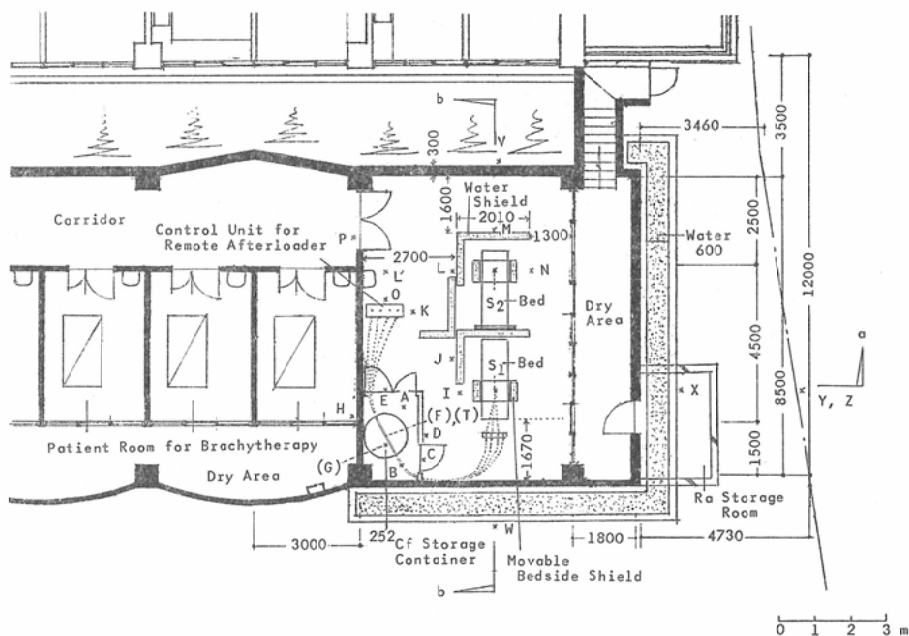


Fig. 1. Diagram of the  $^{252}\text{Cf}$  storage and treatment facility and its environs

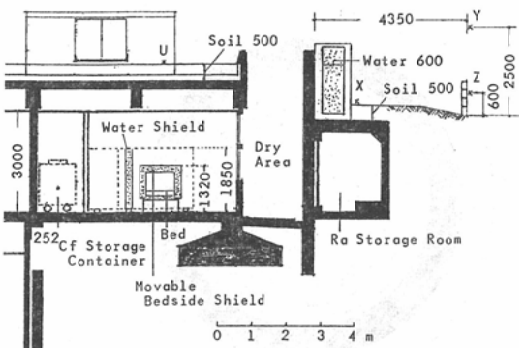


Fig. 2. a—a section of the  $^{252}\text{Cf}$  storage and treatment facility in Fig. 1

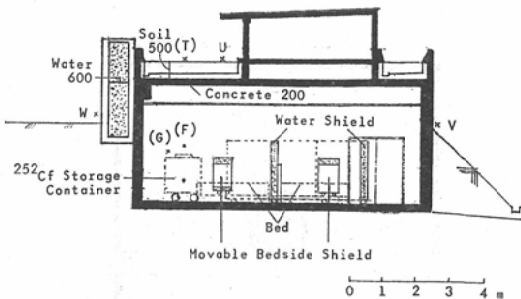


Fig. 3. b—b section of the  $^{252}\text{Cf}$  storage and treatment facility in Fig. 1

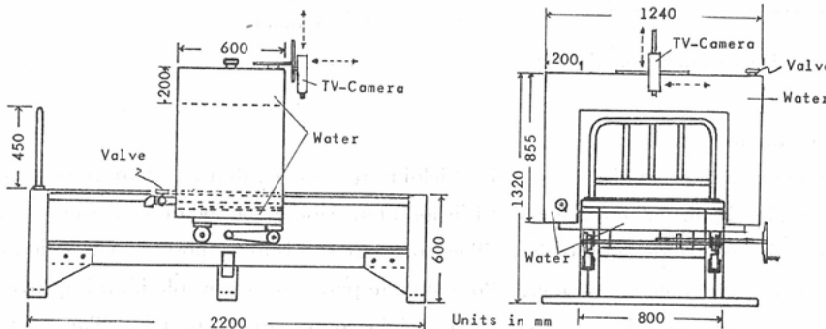


Fig. 4. Treatment bed for remote afterloading therapy

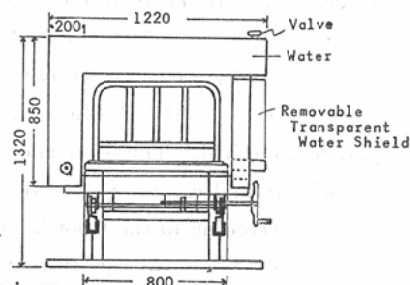
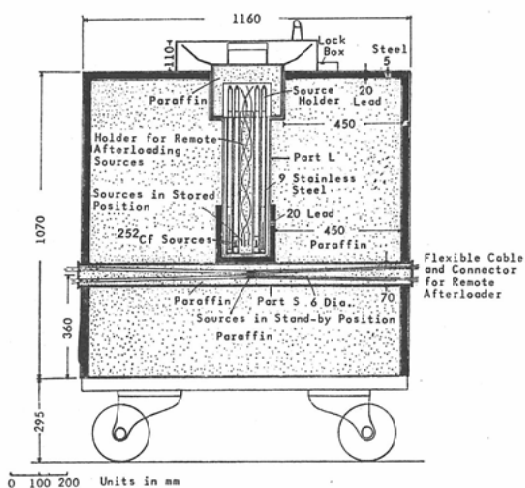
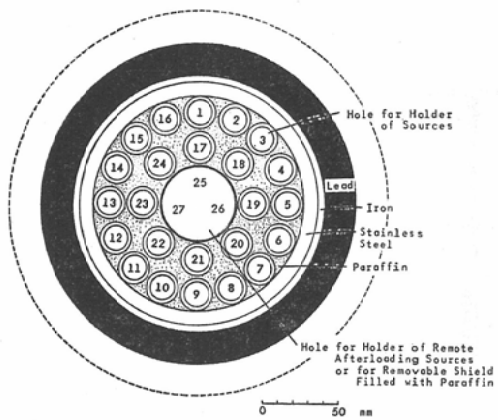


Fig. 5. Treatment bed for interstitial therapy

slides easily on a rail from one end of the bed to the other as shown in Figs. 4 and 5. A TV camera for confirming the position of source is mounted on the bed for remote afterloading therapy shown in Fig. 4. A removable transparent shield is placed on one side of the bed for the interstitial therapy shown in Fig. 5. The therapist can insert the seed assemblies into the guide tube while observing the patient behind the shield. Pulse and temperature checks of the patient can be made at the nurse station with a remote control unit connected to each bed, and the patients can also be observed at the nurse station with a TV camera installed in the treatment rooms. This remote control system for patient care is applied for all brachytherapy patients.

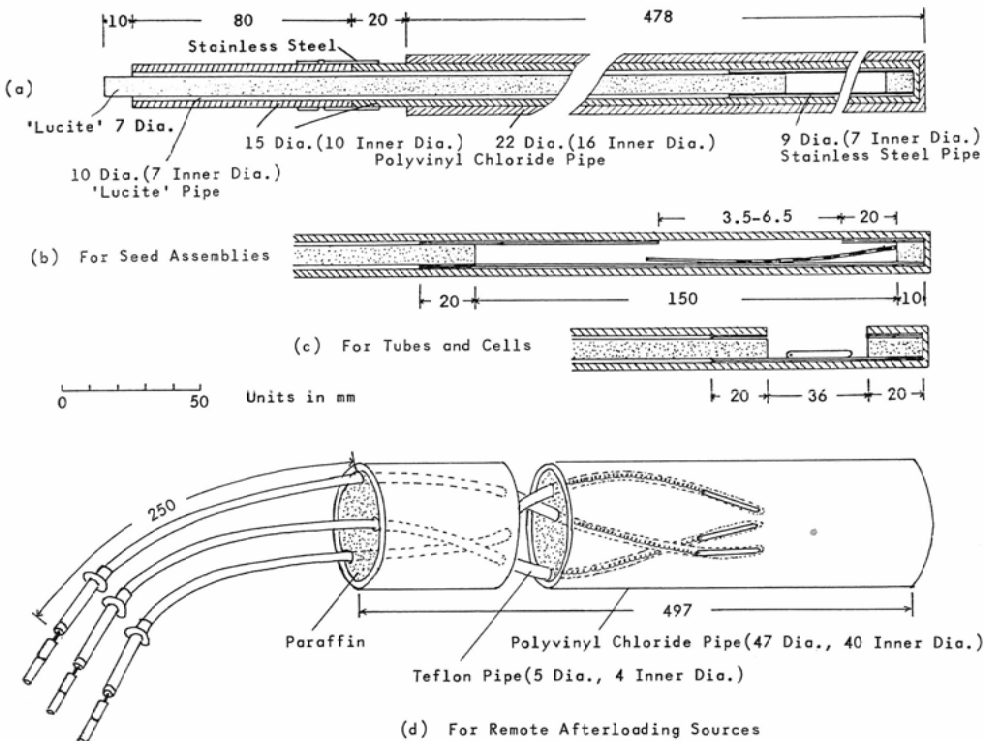
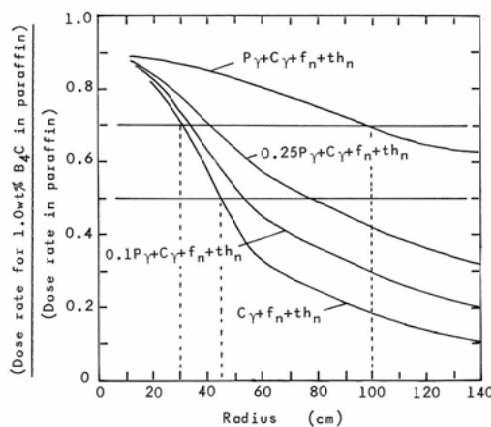
Fig. 6.  $^{252}\text{Cf}$  storage containerFig. 7. Cross section of part L of  $^{252}\text{Cf}$  storage container

### 3. Storage container

The storage container consists of a main shielding part of paraffin and two source storage parts, L and S, as shown in Fig. 6. The storage part L is for a long storage period of seed assemblies, afterloading cells, and tubes for the remote afterloader. The storage part S is for a short storage period of the sources during the use as the remote afterloader. Both storage parts are removable if an improvement of these parts is necessary. Figure 7 shows a cross section of the source storage part L. The small holes are for source holders of seed assemblies and afterloading cells and tubes, and the large hole is for the holder of sources connected to a source cable for the remote afterloader or for the removable shield filled with paraffin. These holders are shown in Fig. 8. The large hole can also be used to irradiate materials and small animals by radiation from the sources of surrounding holes.

The primary shield material chosen for the storage was paraffin with lead in the innermost and outermost part of the shield. The inner and the outer lead provide attenuation of the primary  $\gamma$ -rays and both the primary and capture  $\gamma$ -rays, respectively. Boron-10 was not added to paraffin to reduce the capture  $\gamma$ -rays according to the following considerations.

The effect of the addition of  $\text{B}_4\text{C}$  to paraffin was calculated with varying amounts of  $\text{B}_4\text{C}$ , thicknesses of paraffin, and transmission rates of primary  $\gamma$ -rays based on the data of Stoddard and Hootman.<sup>10)</sup> The effect of  $\text{B}_4\text{C}$  on total dose is dominant when the thickness of paraffin is great and transmission rate of primary  $\gamma$ -rays is small, but this effect does not change significantly with the amount of  $\text{B}_4\text{C}$  when the amount is greater than 1% by weight. Figure 9 shows the effect of the addition of 1 wt%  $\text{B}_4\text{C}$  to paraffin with varying thickness of paraffin when the transmission rate of primary  $\gamma$ -rays is 1, 0.25, 0.1, or 0. The ordinate is the ratio of total dose rates with and without boron addition. At thicknesses up to about 45 cm, the addition of  $\text{B}_4\text{C}$  does not reduce the total dose rate significantly if the transmission rate of primary  $\gamma$ -rays is greater than 0.25, which is the transmission rate obtained with a 2-cm lead. This is the primary reason for not adding  $\text{B}_4\text{C}$  to paraffin. The other reasons are that it is difficult to distribute  $\text{B}_4\text{C}$  uniformly in paraffin, and the total neutron dose rate in the shield of 1 wt%  $\text{B}_4\text{C}$  in paraffin is greater than

Fig. 8. Holders for various  $^{252}\text{Cf}$  sourcesFig. 9. Effect of addition of 1 wt%  $\text{B}_4\text{C}$  to paraffin on total dose rate with varying thickness of paraffin.  $\text{P}_\gamma$ : primary  $\gamma$  rays,  $\text{C}_\gamma$ : capture  $\gamma$  rays,  $\text{f}_n$ : fast neutrons,  $\text{th}_n$ : thermal neutrons.

that in paraffin shield when the thickness of both shields is the same, as shown in Table 1.

#### 4. Remote afterloader

The remote afterloading unit for the intracavitary therapy consists of  $^{252}\text{Cf}$  tubes connected to the source cables, a source storage container, a control unit, applicators, flexible supply tubes, and drive

cables, a supporting unit for applicators and supply tubes, and the bed for treatment. The constitution of this unit is similar to that of other units<sup>4-9)</sup> except for a few points.

When the sources are used for the remote afterloader, they are attached to the drive cables, which are connected to the storage container from the control unit, and are stored at the stand-by position in the part S of storage container shown in Fig. 6 during setting up of the applicators within the patient. The applicators for the ovoids and uterine canal are similar to the TAO applicators, which were developed for radium therapy by Drs. Tazaki, Arai, and Oryu.<sup>2)</sup> After the patient is ready for treatment, the sources are driven out of the storage container to the end of the applicator within the patient by the manual control handles attached to the control unit, which is situated outside the treatment room. Source position indicators, which are mechanically linked to the drive cable, show the position of the source at any instant of time. The sources are brought to rest at the far end of the applicator by the action of mechanical stops attached to the source cable. The "on" and the "off" position of the sources are indicated by red and green lights, respectively.

The source may be drawn back to a prescribed distance from the end of the applicator by the manual control handle, observing the scales on the source cable and its transparent guide tube of the applicator with the TV camera attached to the treatment bed, if necessary. In this case the lights do not indicate the position of the source, but the radiation monitor installed in the treatment room indicates it.

When it is necessary to store the sources for a long period, the supply tubes are connected to the part L of the storage container, and then the sources are moved from the stand-by position in the part S

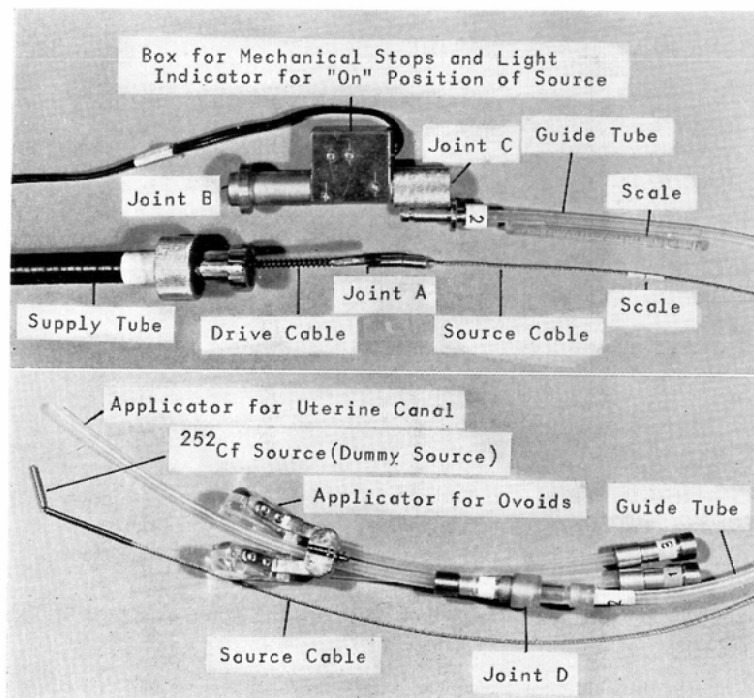


Fig. 10. Accessories for the remote afterloader

to the stored position in the part L by the remote control handles. After that, the source cables connected to the drive cables are removed at the joint A shown in Fig. 10.

### 5. Design radiation levels

When 100- $\mu\text{g}$   $^{252}\text{Cf}$  sources are stored in the storage container, radiation levels for the mixed neutron-gamma field from  $^{252}\text{Cf}$  are less than 2 mrem/h at any position outside the storage room. When 100- $\mu\text{g}$   $^{252}\text{Cf}$  sources are used in two treatment rooms, the radiation levels are less than 2 mrem/h at the position of the control unit of the remote afterloader, in the corridor, and in the adjacent radiotherapy patient room, and less than 0.06 mrem/h in the road outside the hospital.

### Shielding Calculations and Survey Results

For the design dose calculation of the storage room, it was assumed that there were 100  $\mu\text{g}$  of  $^{252}\text{Cf}$  sources in the center of the storage container. The points of calculation are shown by letters in Figs. 1 and 3. For the treatment room, it was assumed that there were 60  $\mu\text{g}$  of  $^{252}\text{Cf}$  at the position  $S_1$  of the treatment bed for the remote afterloading therapy and 40  $\mu\text{g}$  of  $^{252}\text{Cf}$  at the position  $S_2$  of the treatment bed for the interstitial therapy. The points of calculation are shown in Figs. 1, 2, and 3.

The primary source of shielding information was the “ $^{252}\text{Cf}$  Shielding Guide” by Stoddard and Hootman.<sup>10)</sup> The Guide does not contain data for composite shields of lead followed by paraffin or interaction of neutrons in lead, and for slab shields. In the shielding calculations for the slab shields with a large area, the data for spherical shields were used, because the data for a slab shield are close to the data for a spherical shield as the area of the shielding material increases.<sup>11)</sup> For the movable bedside shield, the data for slab shields<sup>11)</sup> were applied.

Contributions to the calculated total dose rate include primary and capture  $\gamma$ -rays interacting with paraffin, water, concrete, lead, and soil, and thermal and fast neutrons interacting with paraffin, water,

Table 1. Dose equivalent rates at 100 cm from 100  $\mu\text{g}$   $^{252}\text{Cf}$  in stored position of part L in Fig. 6

	P		PB
	Calc. dose rate (mrem/h)	Meas. dose rate (mrem/h)	Calc. dose rate (mrem/h)
Fast neutrons	0.343	$0.51 \pm 0.20^*$ $0.17 \pm 0.05^{**}$	0.439
Thermal neutrons	0.0382	0.01	0.00134
Primary $\gamma$ -rays	0.239		0.358
Capture $\gamma$ -rays	0.668	$0.79 \pm 0.05$	0.239
Total	1.29	$1.30 \pm 0.21^*$ $0.96 \pm 0.07^{**}$	1.04

P: 45-cm radius paraffin cylindrical shield

+ 2 cm Pb in innermost part + 2 cm Pb in outermost part

PB: 45-cm radius paraffin cylindrical shield with 1 wt%  $\text{B}_4\text{C}$

+ 2 cm Pb in innermost part + 2 cm Pb in outermost part

measured values: \*neutron-rem dose ratemeter; \*\*Kodak NTA film, exposure time

234 h; thermal neutrons EON thermal dosimeter, exposure time 90 h;  $\gamma$ -rays G-M counter

detector—floor distance 78 cm

Table 2. Radiation levels for 100  $\mu\text{g}$   $^{252}\text{Cf}$  in stored position of part L in Fig. 6

Position keyed to diagram (Figs. 1 and 2)	Distance from source (cm)	Dose equivalent rate (mrem/h)					
		Neutrons		Gamma rays		Total	
		Calc.	Meas.	Calc.	Meas.	Calc.	Meas.
A	100	0.381	$0.51 \pm 0.20^*$ $0.17 \pm 0.05^{**}$	0.910	$0.79 \pm 0.05$	1.29	$1.30 \pm 0.21^*$ $0.96 \pm 0.07^{**}$
B	100	0.381	$0.65 \pm 0.41^*$ $0.16 \pm 0.04^{**}$	0.910	$0.71 \pm 0.03$	1.29	$1.36 \pm 0.41^*$ $0.87 \pm 0.05^{**}$
C	120	0.263	$0.60 \pm 0.41^*$ $0.09 \pm 0.04^{**}$	0.628	$0.63 \pm 0.05$	0.891	$1.23 \pm 0.41^*$ $0.72 \pm 0.06^{**}$
D	103	0.305	$0.51 \pm 0.34^*$ $0.08 \pm 0.03^{**}$	0.317	$0.40 \pm 0.04$	0.622	$0.91 \pm 0.34^*$ $0.48 \pm 0.04^{**}$
E	130	0.225	$0.70 \pm 0.31^*$ $0.04 \pm 0.02^{**}$	0.538	$0.45 \pm 0.06$	0.763	$1.15 \pm 0.32^*$ $0.49 \pm 0.06^{**}$
F	100***	(0.572)	$2.71 \pm 0.59^*$ $(5.70)$	6.04	$\pm 0.14$	(6.27)	$8.75 \pm 0.61^*$
F	100****	(1.05)	$2.73 \pm 0.58^*$ $(5.41)$	5.11	$\pm 0.22$	(6.46)	$7.84 \pm 0.62^*$ $5.63 \pm 0.24^{**}$
G	100	0.381	$0.93 \pm 0.32^*$	1.62	$1.07 \pm 0.05$	2.00	$2.00 \pm 0.32^*$
H	88	0.418	$0.67 \pm 0.48^*$	0.434	$0.34 \pm 0.04$	0.852	$1.01 \pm 0.48^*$
T	350***	(0.019)	—	(0.094)	—	(0.113)	—
	****	(0.034)	—	(0.089)	—	(0.123)	—

\*measured by the neutron-rem dose ratemeter

\*\*measured by the Kodak NTA film (exposure time 234 h)

\*\*\*stored 60  $\mu\text{g}$   $^{252}\text{Cf}$  in large hole and 40  $\mu\text{g}$   $^{252}\text{Cf}$  in small holes\*\*\*\*stored 100  $\mu\text{g}$   $^{252}\text{Cf}$  in small holes

detector—floor distance 78 cm

concrete, and soil. Attenuation of neutrons in lead and iron was not considered. For concrete and soil, the data for concrete-01 and for Nevada Test Site soil (dry) in the  $^{252}\text{Cf}$  Shielding Guide were used, respectively.

Tables 1, 2, 3, and 4 give the results of the design calculations. In these calculations, following values were used<sup>10)</sup>:

Neutron emission rate	$2.4 \times 10^6 \text{ n s}^{-1} \mu\text{g}^{-1}$
Neutron dose equivalent rate in air at 1 m	2.33 mrem $\text{h}^{-1} \mu\text{g}^{-1} \text{m}^2$
Gamma dose rate in air at 1 m	0.164 mrad $\text{h}^{-1} \mu\text{g}^{-1} \text{m}^2$
Effective half life	2.65 years

The radiation protection survey of the completed facility was performed in three parts: Case (1) with 75  $\mu\text{g}$  of  $^{252}\text{Cf}$  in the stored position of part L, Case (2) with three 15- $\mu\text{g}$  tubes in the stand-by position of part S and totaling 30  $\mu\text{g}$  of seed assemblies and cells in the stored position of part L, and Case (3) with three 15- $\mu\text{g}$  tubes on the bed for the remote afterloading therapy and totaling 30  $\mu\text{g}$  of seed assemblies and cells on the bed for interstitial therapy. A neutron-rem dose ratemeter with a scintillation crystal  $^6\text{LiI}(\text{Eu})$  inserted into a 20-cm moderator-absorber (polyethylene-cadmium) sphere, manufactured by the Laboratorium Prof. Dr. Berthold in Germany, and Kodak NTA films, which were calibrated in air with  $^{252}\text{Cf}$  neutrons, were used for neutron measurements. A G-M counter, calibrated in air with radium, was used for gamma measurements. The direct-reading thermal neutron dosimeter of EON Inc., U.S.A.,

Table 3. Radiation levels for  $60 \mu\text{g}^{252}\text{Cf}$  in stand-by position of part S and  $40 \mu\text{g}^{252}\text{Cf}$  in stored position of part L in Fig. 6

Position keyed to diagram (Figs. 1 and 2)	Distance from source (cm)		Dose equivalent rate (mrem/h)					
			Neutrons		Gamma rays		Total	
	L	S	Calc.	Meas.	Calc.	Meas.	Calc.	Meas.
A	100	100	0.381	$0.51 \pm 0.12^*$ $0.15 \pm 0.05^{**}$	1.34	$0.89 \pm 0.17$	1.72	$1.40 \pm 0.21^*$ $1.04 \pm 0.18^{**}$
B	100	100	(0.381)	$1.64 \pm 0.85^*$ $0.48 \pm 0.12^{**}$	(4.27)	$0.99 \pm 0.03$	(4.65)	$2.63 \pm 0.85^*$ $1.47 \pm 0.12^{**}$
C	120	120	0.263	$0.78 \pm 0.54^*$ $0.22 \pm 0.09^{**}$	0.925	$0.86 \pm 0.08$	1.19	$1.64 \pm 0.55^*$ $1.08 \pm 0.12^{**}$
D	103	103	0.305	$0.63 \pm 0.44^*$ $0.11 \pm 0.06^{**}$	0.467	$0.54 \pm 0.05$	0.772	$1.17 \pm 0.44^*$ $0.65 \pm 0.08^{**}$
E	130	130	0.225	$0.54 \pm 0.28^*$ $0.08 \pm 0.06^{**}$	0.793	$0.44 \pm 0.09$	1.02	$0.98 \pm 0.29^*$ $0.52 \pm 0.11^{**}$
F	100	110	(0.546)	$1.46 \pm 0.39^*$ $0.50 \pm 0.11^{**}$	(2.90)	$1.81 \pm 0.03$	(3.45)	$3.27 \pm 0.39^*$ $1.31 \pm 0.11^{**}$
G	100	110	0.341	$0.82 \pm 0.60^*$ $0.11 \pm 0.05^{**}$	1.10	$0.77 \pm 0.03$	1.44	$1.59 \pm 0.60^*$ $0.88 \pm 0.06^{**}$
H	88	88	0.417	$0.69 \pm 0.47^*$	0.640	$0.30 \pm 0.02$	1.06	$0.99 \pm 0.47^*$
T	350	360	(0.0186)	—	(0.0494)	—	(0.068)	—

\*measured by the neutron-rem dose ratemeter

\*\*measured by the Kodak NTA film (exposure time 191 h)

detector—floor distance 66 cm

Table 4. Radiation levels for  $60 \mu\text{g}^{252}\text{Cf}$  at  $S_1$  and  $40 \mu\text{g}^{252}\text{Cf}$  at  $S_2$  in Fig. 1

Position keyed to diagram (Figs. 1, 2 and 3)	Distance from source (cm)		Dose equivalent rate (mrem/h)					
	$S_1$	$S_2$	Calc.	Meas.*	Calc.	Meas.	Calc.	Meas.
H	420	580	0.66	$0.50 \pm 0.51$	0.13	$0.08 \pm 0.01$	0.79	$0.58 \pm 0.51$
I	100	360	12.2	$17.4 \pm 2.2$	7.3	$3.96 \pm 0.04$	19.5	$21.4 \pm 2.2$
J	150	300	6.29	$3.80 \pm 1.07$	3.39	$1.55 \pm 0.02$	9.68	$5.35 \pm 1.07$
K	340	260	1.79	$2.99 \pm 1.39$	0.93	$0.54 \pm 0.01$	2.72	$3.53 \pm 1.39$
L	370	130	1.23	$1.85 \pm 0.73$	1.83	$1.19 \pm 0.02$	3.06	$3.04 \pm 0.73$
L'	470	320	0.16	$2.49 \pm 1.22$	0.32	$0.47 \pm 0.01$	0.48	$2.96 \pm 1.22$
M	470	120	10.2	$6.45 \pm 1.48$	3.8	$2.16 \pm 0.03$	14.0	$8.61 \pm 1.48$
N	360	100	9.0	$27.1 \pm 3.8$	4.4	$3.42 \pm 0.04$	14.4	$30.5 \pm 3.8$
O	430	320	0.14	$2.89 \pm 1.14$	0.31	$0.43 \pm 0.01$	0.45	$3.32 \pm 1.14$
P	600	420	0.08	$1.28 \pm 0.69$	0.18	$0.22 \pm 0.03$	0.26	$1.50 \pm 0.69$
U	340	480	1.39	—	0.18	—	1.57	—
V	690	360	0.40	—	0.11	—	0.51	—
W	410	740	0.0007	—	0.017	—	0.018	—
X	550	650	0.0006	—	0.0081	—	0.0087	—
Y	930	1020	0.00001	—	0.0012	—	0.0012	—
Z	890	950	0.00001	—	0.00010	—	0.00010	—

\*measured by the neutron-rem dose ratemeter

detector—floor distance 80 cm

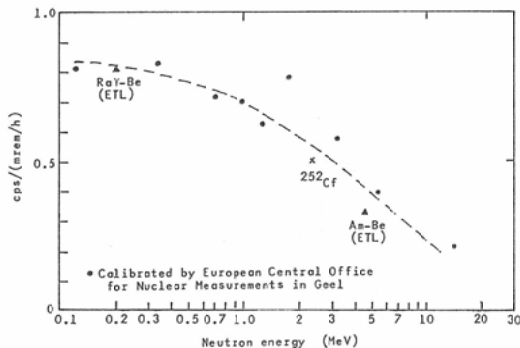


Fig. 11. Neutron energy dependence of neutron-rem dose  
ratemeter LB6603-1 manufactured by the Laboratorium Prof.  
Dr. Berthold

calibrated by the Electrotechnical Laboratory (ETL) of Japan, was used for thermal neutron measurements.

Tables 1, 2, 3, and 4 give the results of measurements. The measured values in Tables 1 and 2, in Table 3, and in Table 4 were converted to values for 100- $\mu$ g  $^{252}\text{Cf}$  sources, for 40  $\mu$ g in part L and 60  $\mu$ g in part S, and for 60  $\mu$ g at S<sub>1</sub> and 40  $\mu$ g at S<sub>2</sub>, respectively.

Measured neutron dose equivalent rates with a neutron-rem dose ratemeter were higher than those with NTA films at low radiation levels. This difference is probably due to the fact that the rem-dose ratemeter over-responds at low neutron energies as shown in Fig. 11 and that the NTA film does not respond to neutrons with energies between about 10 eV and 0.5 MeV.<sup>12)</sup>

Measured neutron dose equivalent rate at position L' was 1.4 of that at position L, while calculated value at L' was 0.13 of that at L. This may be due to the difference of the scattered neutrons at both points from the floor, ceiling, and wall, because the use of 10-cm thick water tank under the source can be reduced the neutron dose rate at L' by a factor of 2.

### Discussion and Conclusion

Applicability of the Guide by Stoaddrd and Hootman for the spherical shields was confirmed by the present design calculations and radiation protection survey. However, for local shielding such as the bedside shielding, which is preferable rather than structural shielding for protection against radiation from brachytherapy sources, the Guide cannot be applied, because scattered neutrons from the floor, ceiling, and wall may reach behind the shield.

By using the remote afterloader, radiation exposure to staff for the intracavitary therapy may be reduced significantly, while by the present afterloading technique for the interstitial therapy neutron dose to the therapist is 1 to 2 mrem/ $\mu$ g of  $^{252}\text{Cf}$  implanted.<sup>13)14)</sup> In the future, remote interstitial implantation method will be needed.

This work was supported in part by the U.S. Department of Energy under Contract No. EY-76-C-09-0739 and by Grants-in-Aid for Cancer Research from the Ministry of Education, Science and Culture, and from the Ministry of Health and Welfare, Japan, which are gratefully acknowledged.

## References

- 1) Henschke, U.K., Hilaris, B.S. and Mahan, G.D.: Afterloading in interstitial and intracavitary radiation therapy. *Am. J. Roentgenol.*, 90: 386—395, 1963
- 2) Tazaki, E., Arai, T. and Oryu, S.: A new applicator for uterine cervical cancer. *Rinsho-Hôshasen*, 10: 768—775, 1965
- 3) Paine, C.H.: Modern after-loading methods for interstitial radiotherapy. *Clin. Radiol.*, 23: 263—272, 1972
- 4) Walstam, R.: Remotely-controlled afterloading radiotherapy apparatus (a preliminary report). *Phys. Med. Biol.*, 7: 225—228, 1962
- 5) Henschke, U.K., Hilaris, B.S. and Mahan, G.D.: Remote afterloading with intracavitary applicators. *Radiology*, 83: 344—345, 1964
- 6) O'Connell, D., Howard, N., Joslin, C.A.F., Ramsey, N.W. and Liversage, W.E.: A new remotely controlled unit for the treatment of uterine carcinoma. *Lancet*, 2: 570—571, 1965
- 7) Wakabayashi, M., Irie, G., Sugawara, T., Mitsuhashi, H., Yamaguchi, S., Omoe, K., Hanajima, N., Kato, S., Matsuda, S., Inui, Y., Tajika, K. and Hirayama, Y.: Trial construction of remote afterloading unit. *Rinsho-Hôshasen*, 11: 678—684, 1966
- 8) Yamashita, H. and Makino, S.: Remotely controlled afterloading apparatus. *Aust. Radiol.*, 16: 421—426, 1972
- 9) Wada, T.: Fundamental aspects of neutron radiotherapy with a  $^{252}\text{Cf}$  source. 1. Radiation protection of  $^{252}\text{Cf}$  remote afterloading apparatus. *Keio Igaku*, 54: 387—395, 1977
- 10) Stoddard, D.H. and Hootman, H.E.:  $^{252}\text{Cf}$  Shielding Guide, DP-1246, pp. 56—62, 1971, Savannah River Laboratory, Aiken, South Carolina
- 11) Onai, Y., Irfune, T., Tomaru, T. and Uchida, I.: Attenuation curves for  $^{252}\text{Cf}$  radiation in slab shields. *Radioisotopes*, 24: 232—234, 1975
- 12) ICRU: ICRU Rep. 20, Radiation Protection Instrumentation and Its Application. p. 34, 1971, International Commission on Radiation Units and Measurements, Washington, D.C.
- 13) Oliver, G.D.: Aspects of radiation control for clinical implants to californium-252. *Health Phys.*, 23: 187—192, 1972
- 14) Tsuya, A., Kaneta, K., Onai, Y., Irfune, T. and Tomaru, T.: Clinical experience with californium-252 (first report). *Nippon Acta Radiol.*, 37: 238—247, 1977